REVISTA DE
ARQUITETURA IMED

Acceleration of cements with phosphogypsum through sodium chloride: analysis of compressive strength and corrosive potential

Aceleração de cimentos à base de fosfogesso utilizando cloreto de sódio: análise da resistência à compressão e potencial corrosivo

Matheus Henrique Gomes de Medeiros(1); Caroline Vieira Alves Alves(2); Rayara Pinto Costa(3); Ana Paula Kirchheim(4); Seiiti Suzuki(5)

1 Doutorando em Engenharia Civil, EE – UFRGS. ORCID: https://orcid.org/0009-0001-5029-7397 | E-mail: matheus96h@gmail.com
2 Engenharia Civil, EE – UFRGS. E-mail: carolvieiralves_25@hotmail.com
3 Doutoranda em Engenharia de Materiais, EE – UFRGS. ORCID: https://orcid.org/0000-0003-3077-3314 | E-mail: rayarapintocosta@gmail.com
4 Professora em Engenharia Civil, EE – UFRGS. ORCID: https://orcid.org/0000-0002-8241-0331 | E-mail: anapaula.k@gmail.com
5 Mestre em Engenharia Civil, IPT – SP. ORCID: https://orcid.org/0000-0003-1252-5034 | E-mail: seiitis@intercement.com

Revista de Arquitetura IMED, Passo Fundo, vol. 13, n. 1, p. 92-115, janeiro-junho, 2024 - ISSN 2318-1109

DOI: https://doi.org/10.18256/2318-1109.2024.v13i1.5066

Sistema de Avaliação: *Double Blind Review*

Como citar este artigo / How to cite item: clique aqui!/click here!

Resumo

Phosphogypsum, a byproduct of phosphoric acid production in the fertilizer industry, is an environmentally friendly source of calcium sulfate for controlling the setting time in cements, replacing gypsum. However, as it is a waste product, it can contain impurities such as F- and P2O5, which may prolong the setting time beyond the desired duration and reduce initial mechanical strength. A solution to this problem is the use of hydration/strength accelerators, of which several types are available. Considering cost, sodium chloride can be an attractive option. However, it is known that chlorides can cause corrosion in reinforcements. Therefore, the incorporation of these materials as setting accelerators in concrete requires caution regarding the durability of structures. This study aims to analyze the influence of using phosphogypsum in Portland cements and the impact of sodium chloride as an accelerator. Tests were conducted to verify the behavior of the mixtures at early ages, using isothermal calorimetry in pastes, compressive strength, and corrosion potential in concretes. The results confirm that the presence of phosphogypsum delays the setting process but does not significantly affect the final strengths. Additionally, the tested chloride levels did not indicate a high probability of reinforcement corrosion.

Palavras-chave: Fosfogesso; Cloreto de Sódio; Tempo de Pega; Resistência Mecânica; Corrosão

Abstract

O fosfogesso, um subproduto da produção de ácido fosfórico na indústria de fertilizantes, é uma fonte ambientalmente amigável de sulfato de cálcio para o controle do tempo de pega em cimentos, substituindo a gipsita. Contudo, por ser um resíduo, pode conter impurezas como F^- e P_2O_5, que podem prolongar o tempo de pega além do desejado e reduzir a resistência mecânica inicial. Uma solução para esse problema é o uso de aceleradores de hidratação/resistência, dos quais existem vários tipos disponíveis. Considerando o custo, o cloreto de sódio pode ser uma opção atrativa. No entanto, é conhecido que os cloretos podem causar corrosão em armaduras. Portanto, a incorporação desses materiais como aceleradores de pega em concretos exige cuidados em relação à durabilidade das estruturas. Este trabalho busca analisar a influência do uso de fosfogesso em cimentos Portland e o impacto do cloreto de sódio como acelerador. Foram realizados testes para verificar o comportamento das misturas nas primeiras idades, utilizando calorimetria isotérmica em pastas, resistência à compressão e potencial de corrosão em concretos. Os resultados confirmam que a presença de fosfogesso retarda o processo de pega, mas não afeta significativamente as resistências finais. Além disso, os níveis de cloretos testados não indicaram alta probabilidade de corrosão das armaduras.

Keywords: Phosphogypsum; Sodium Chloride; Setting Time; Mechanical Strength; Corrosion

1 Introduction

Generally, natural gypsum (NG) is incorporated in Portland cement production as an SO_3 source to control setting time, delaying the start of clinker solidification upon contact with water (Kirchheim *et al*., 2010; Mehta; Monteiro, 2014). The main global producers of gypsum are the United States, Iran, and Canada (Baltar; Luz; Bastos, 2004). In Brazil, the state of Pernambuco accounts for 95% of national production, with deposits in the Araripe region considered the highest quality in the world (Costa *et al*., 2022; Cui *et al*., 2023; Haneklaus *et al*., 2022). However, due to Brazil's vast territory, supplying gypsum to cement plants in the Central-West, Southeast, and South regions is expensive and environmentally harmful due to long distances (Canut *et al*., 2008; Costa *et al*., 2022).

An alternative to using gypsum in the cement industry is phosphogypsum (PG), a by-product of phosphoric acid production in the agricultural fertilizer industry. For every ton of phosphoric acid produced, four to six tons of PG are generated (Rashad, 2017). Global PG production is estimated at 200 million tons per year, with Brazil contributing up to 5.6 million tons (Silva; Giulietti, 2010; Hermann; Kraus; Hermann, 2018). This production is expected to increase, possibly reaching between 200 and 250 million tons over the next two decades (IAEA, 2013).

However, PG disposal is a significant concern. Kuzmanović (2020) notes that only 15% of global production is recycled for construction materials, while 85% is discarded outdoors without treatment, causing water, soil, and air pollution and affecting human health (Akfas *et al*., 2024; Canut *et al*., 2008). These facts underscore the need to increase PG use in construction. The presence of calcium sulfate allows the material to replace gypsum, especially in industrial plants far from the gypsum-producing center. However, impurities in PG can have undesired effects, such as excessively delaying setting time and initial concrete strengths (Shen, 2012; Canut *et al*., 2008; Costa *et al*., 2022).

Islam (2017) suggests that additions of more than 2% PG significantly increase setting time due to minor phosphorus and fluorine components. Andrade Neto *et al.* (2021a) reported hydration delays and lower mechanical strength in mortar with PG compared to gypsum mixes. Shen *et al.* (2012) also observed significant delays in setting time attributed to phosphorus presence.

To mitigate the negative effects of PG, one solution is to use reaction accelerators, which reduce setting time and/or increase initial compressive strength (Myrdal, 2007). Lee, Lee and Kim (2020) classify these accelerators into two groups: setting and strength accelerators, based on the heat release characteristics of the cement-water reaction. There are two types of strength accelerators: water-soluble inorganic salts and organic chemicals (Ren *et al*., 2021). Water-soluble inorganic salts, such as calcium chloride, are effective in improving initial strength (Lee; Lee; Kim, 2020).

Sodium chloride (NaCl) is also effective, being a cheap and readily available alternative (Bauer, 2000). However, when using chloride-based accelerators, there is concern about reinforcing steel corrosion. Therefore, it is essential to conduct evaluative studies when considering sodium chloride as a mitigator of PG effects (Ribeiro; Cunha, 2014).

In this regard, Ribeiro and Cunha (2014) present the electrochemical potential test as a measure of the likelihood of a metal reacting with its surrounding environment. In reinforced concrete, it pertains to the reaction of reinforcement with concrete electrolyte. This method seeks to delineate zones of different potentials indicating areas of steel behavior. ASTM C876 (ASTM, 2015) defines the probability of reinforcing steel corrosion based on potential value ranges.

This study aims to identify the influence of chlorides as reaction accelerators in PG cements, aiming to enable the total or partial replacement of gypsum with PG in Portland cement production. The cements hydration were analyzed in pastes, the compressive strength in concrete, and the corrosion potential in reinforced concrete specimens.

2 Materials and method

2.1 Physical-chemical characterization of raw materials

2.1.1 Cement

In this research, three "CP V-ARI RS" cements, industrially produced for research purposes by a partnering cement industry, were used. In the production of these cements, clinker and three sources of calcium sulfate were employed respectively, named 100% gypsum (NG); 50% gypsum (NG) and 50% phosphogypsum (PG); 100% phosphogypsum (PG). PG was neutralized by the cement producer with 5% hydrated lime (by mass %) according to Andrade Neto et al. (2021). The cements were evaluated for initial setting time in minutes, NBR 16607 (ABNT, 2018); final setting time in minutes, NBR 16607 (ABNT, 2018); water required for normal consistency paste, NBR 16606 (ABNT, 2019a); loss on ignition (%), NM18 (AMN, 2012); #200 - percentage retained on 75 μm sieve, NBR 11579 (ABNT, 2015b); Blaine - Determination of fineness by Air Permeability Method in m2/kg, NBR 16372 (AMN, 1996); and compressive strength at ages 01, 07, and 28 days, NBR 7215 (ABNT, 2019b). Additionally, the chemical composition of the cements was evaluated by X-ray fluorescence (XRF).

2.1.3 Source of Cl^-

To accelerate the reactions of initial and final setting times and analyze the early-age behavior of concretes through mechanical strength, three chloride ion (Cl-)

contents were added to the mixtures using analytical grade sodium chloride (NaCl). The choice of chloride contents was based on NBR 12655 (ABNT, 2015), which specifies maximum chloride ion contents for different environmental classes. Thus, these limits were used as parameters to define the contents: 0% (I), 0.15% (II), and 0.30% (III) of chloride ions relative to the mass of cement. The cement paste ID for each cement type and chloride content is described in Table 1.

Table 1 – Samples identification

ID	Description
CEM I –I	Clinker; 100% NG; 0% Cl^-
CEM I –II	Clinker; 100% NG; 0.15% Cl^-
CEM I –III	Clinker; 100% NG; 0.3% Cl^-
CEM II-I	Clinker; 50% NG and 50%PG; 0% Cl^-
CEM II-II	Clinker; 50% NG and 50%PG; 0.15% Cl^-
CEM II-III	Clinker; 50% NG and 50%PG; 0.3% Cl^-
CEM III-I	Clinker; 100% PG; 0% Cl^-
CEM III-II	Clinker; 100% PG; 0.15% Cl^-
CEM III-III	Clinker; 100% PG; 0.3% Cl^-

Also, the amount of NaCl required to achieve the desired ion contents was calculated based on the atomic mass, as per Equation 1:

$$0.33\%NaCl = 0.20Cl^- \quad \text{Eq. 1}$$

To verify the possibility of corrosion, two CA50 steel bars with a diameter of 5mm were used as reinforcement in each corrosion potential test specimen. At the ends of the bars, a rigid copper wire with a diameter of 2.5mm was fixed to ensure proper electrical contact. Additionally, all pastes and concretes produced in this study were made with deionized water to prevent any influence on the total chloride ion content, which could be altered by the presence of chemicals used in the treatment of drinking water, such as chlorine.

2.1.2 Agregates

As fine aggregate, dry quartz sand from Rio Jacuí (RS) was used. The particle size distribution of this material was determined according to NBR 248 (ABNT, 2003). Additionally, the specific and bulk densities were determined in accordance with NBR 52 (ABNT, 2009) and NBR 45 (ABNT, 2006), respectively.

The coarse aggregate used in the concrete mixtures was 1-inch basalt gravel sourced from Montenegro (RS). The particle size distribution was determined

according to NBR 248 (ABNT, 2003); bulk density was determined as per NBR 45 (ABNT, 2006); and the shape index was evaluated following NBR 7809 (ABNT, 2019). The aggregates were used in a dry state.

2.2 Mix Design

The concrete mix design was determined based on standard proportions established in preliminary studies, with a fixed cement content of 330 kg/m³. Since no superplasticizing additives were used, the water-to-cement ratio was set at 0.6 (while the commonly practiced ratio in mixes with additives is 0.53). This ratio was verified in previous exploratory tests in the lab, proving suitable for producing cohesive concrete with a slump of 120 mm for the reference mix - 100% gypsum cement without accelerator addition (CEM I-I). The mass proportions are presented in Table 2.

Table 2 – Mix design by weight (kg)

Cement	Sand	Gravel	w/c	NaCl		
				0.0% Cl	0.15% Cl	0.30% Cl
1.000	2.30	3.329	0.6	0	0.00247	0.00494

2.3 Isothermal calorimetry of cement pastes

The cement pastes, in which NG was partially or completely replaced by PG in the presence of chlorides as accelerators, were analyzed for the heat of reaction released. For this purpose, an isothermal calorimetry test was conducted for 72 hours at a constant temperature of 25ºC according to ASTM C1679 (2017). A TAMAir calorimeter from TA Instruments was used with 50 g of cement per sample. Sodium chloride was pre-dissolved in mixing water for five minutes using a magnetic stirrer at medium speed. The mixing procedure involved manual blending of cement with the saline solution for 30 seconds, followed by fixing the cup on the equipment for 20 seconds, and finally electrically mixing the paste in the mixer for 70 seconds, totaling 2 minutes from the start of the reaction.

2.4 Specimens for the corrosion test

The prismatic specimens selected for the corrosion tests were based on the models presented by Cabral (2000), Vieira (2003), and Mota (2016), with dimensions of 65x100x150 mm. Plywood forms were used, and two bars were positioned to divide the height in half. Thus, the top cover depth was less than 30 mm. To standardize external influence conditions, the bars were positioned 30 mm away from the bottom of the form. The schematic diagram is shown in Figure 1.

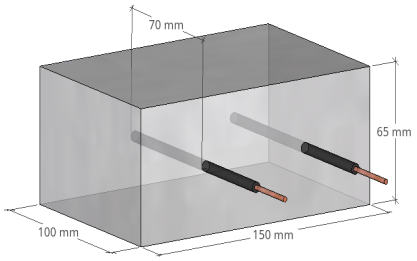

Figure 1 - Sketch of Prismatic Specimen

The steel bars were cut to a length of 120 mm, with 50 mm left exposed externally from the test specimen. Using a bench drill, a hole with a diameter of 2.5 mm and a depth of 10 mm was drilled at the tip of each bar (Figure 2), where copper wires were subsequently inserted. The bars were cleaned to prevent any influence on the results due to initial oxidation processes. For this purpose, the immersion method in a solution of hydrochloric acid and deionized water in a 1:1 ratio, as executed by Vieira (2003), followed by brushing with steel bristles and rinsing with running water, was employed. The bars remained immersed for 10 minutes (Figure 2b). According to Godinho (2018), this procedure is more effective than immersion in acid or brushing alone. Next, the bars were rinsed with isopropyl alcohol to accelerate drying and placed on paper towels, where hot air was blown to ensure complete drying and completion of the cleaning process (Figure 2c).

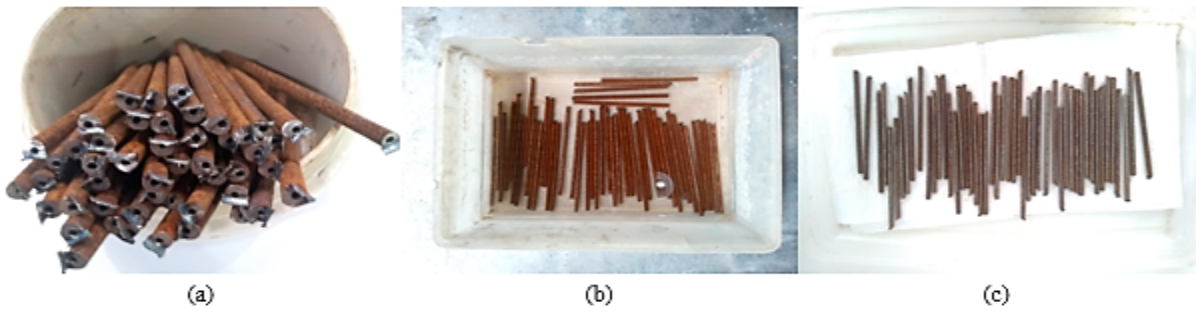

Figure 2 - Preparation of Bars: (a) Cutting and Drilling (b) Immersion in Hydrochloric Acid (c) Dry Bars

After cleaning, the bars were individually wrapped in plastic film until the concrete specimens were cast. Each bar was weighed on a precision scale and identified with the concrete mix design number, followed by letters A or B indicating its position in the mold.

Next, pieces of rigid copper wire, 2.5 mm in diameter, were inserted and soldered to ensure proper electrical contact between the test connector and the reinforcement.

The wire pieces were cut to 40 mm in length, with 30 mm exposed outside the bars. The welding areas and steel were protected with liquid insulating tape, leaving only the copper wire exposed. The finished, identified, and protected bar can be seen in Figure 3.

Figure 3 - Finished Bar

To ensure that the bars remained in place during casting and compaction, PU-type silicone was used to secure them in the correct position inside the molds, aided by styrofoam to hold them in place until the silicone dried. During demolding, the molds were carefully disassembled, and the silicone was removed to release the bars from the mold. Any residual silicone was scraped off with a spatula, and afterward, the exposed parts of the bars were re-covered with liquid insulating tape.

2.5 Concrete casting

For the studies on compressive strength and corrosion potential, nine different concrete mixes were cast, forming specimens for both tests. To dissolve chloride, a mechanical agitator was used for five minutes, following a procedure similar to that used for pastes in section.

Concrete casting was performed using a central shaft mixer, starting with coarse aggregate, followed by initial water, cement, the remaining water, and finally fine aggregate. The complete mixing process for each mix in the mixer lasted between 5 to 6 minutes.

Immediately after mixing, a slump test was conducted to assess the consistency and cohesion of the concrete, following NBR 16889 (ABNT, 2020). Subsequently, the specimens were molded. Both cylindrical and prismatic molds were filled in two layers, each layer compacted on a vibrating table for 10 seconds.

All molds were covered with plastic sheeting to prevent water loss during the initial curing period. After 24 hours, the specimens were demolded, re-identified, and placed in a moist curing chamber (maintained at a constant temperature of 22 ± 2 °C and humidity of 95 ± 2%) for the remainder of the curing process until testing, for both cylindrical and prismatic specimens (Figure 4).

Figure 4 - Cylindrical Specimens (a) and Prismatic Specimens (b): Stored in a Moist Curing Chamber

2.6 Mechanical Compressive Strength

Following the procedure established by NBR 5739 (ABNT, 2018), the cylindrical specimens were subjected to compressive strength testing using an EMIC DL 20000 hydraulic press, equipped with a 200 kN load cell and a loading rate of 0.45 MPa/s. Samples from each mix were tested as follows: 3 specimens at 1 day of age, 3 at 7 days, and 2 at 28 days.

2.7 Corrosion Potential

To analyze the possibility of reinforcement corrosion in the studied concretes due to chloride ion additions, the electrochemical technique of polarization resistance was employed, as proposed by ASTM C876 (ASTM, 2015). A GiII-AC model potentiostat from ACM Instruments, along with Sequencer software for data reading and analysis compatible with the mentioned equipment, was used. The equipment required an Ag/AgCl reference electrode model 3A11 from Analyser. A stainless steel plate was used as the counter electrode positioned below the specimen. To ensure proper electrical contact, sponges moistened with water and soap were placed between the electrode and the specimen, as well as between the specimen and the counter electrode, following the method described by Vieira (2003).

Polarization resistance was conducted by applying a potential variation (ΔE) on the reinforcement from -10 mV to +10 mV, at a rate of 10 mV/min. From this polarization, corrosion potential (Ecorr) values were calculated by the software in relation to the reference electrode used.

Due to the chloride addition in the concretes, immersion cycles in saline solution as described by Vieira (2003), Cabral (2000), and Mota (2016) were not performed. This study aimed to analyze corrosion potential solely due to internal agents, without considering external attacks.

The concrete specimens for corrosion potential analysis (Ecorr) were initially tested at 28 days, followed by weekly potential measurements over two months of testing. Each specimen was tested separately on two bars, resulting in four measurements per mix. Subsequently, the average of these values was calculated. ASTM C 876/15 (2015) establishes ranges of Ecorr values to determine the likelihood of corrosion. Values above -0.85 mV indicate low probability of corrosion (<10%), while values between -0.85 mV and -0.235 mV indicate uncertain probability of corrosion. Values below -0.235 mV suggest high probability of corrosion (>90%), according to the electrode used in the study.

3 Results and discussion

3.1 Physical-chemical characterization of materials

Here are the data related to the characterization of these cements, Table 3 and 4. The chemical composition of each aforementioned cement is presented in Table 4, while other properties of the materials are shown in Table 3. These include: IS (min) - Initial Setting Time in minutes, according to NBR 16607 (ABNT, 2018); FS (min) - Final Setting Time in minutes, according to NBR 16607 (ABNT, 2018); A (%) - Water required for normal consistency paste, according to NBR 16606 (ABNT, 2019a); Loss on Ignition (%) - NM18 (AMN, 2012); #200 - Percentage retained on the 75 μm sieve, according to NBR 11579 (ABNT, 2015b); Blaine - Fineness determination by Air Permeability Method in m2/kg, according to NBR 16372 (AMN, 1996); R1, R2, and R3 (MPa) - Compressive Strength at ages 01, 07, and 28 days, according to NBR 7215 (ABNT, 2019b). The results show that CEM II has an IS approximately 14% higher than CEM III, and 47% higher than CEM I. This behavior suggests that the content of PG, even when treated with 5% hydrated lime, hinders hydration compared to when NG is used. The same trend is observed in the FS of samples. Furthermore, the data indicate that a higher content of PG in the cement reduces the compressive strength at 28 days. Specifically, CEM I has compressive strength values that are 4.3% and 5.48% higher than those of CEM II and CEM III, respectively. The delay in reaction, and consequently in the setting, as well as the compromise of compressive strength, is also observed in studies conducted by Costa (2022), Andrade Neto et al. (2021), and Shen et al. (2012).

Table 3 – Cement characterization

CEM I		**CEM II**		**CEM III**	
IS (min)	170	IS (min)	250	IS (min)	220
FS (min)	230	FS (min)	335	FS (min)	305
A (%)	34.1%	A (%)	33.1%	A (%)	33.0%
LI (%)	4.26	LI (%)	4.12	LI (%)	3.59
#200	0.21	#200	0.21	#200	0.22
Blaine (m^2/kg)	4715	Blaine (m^2/kg)	4980	Blaine (m^2/kg)	4740
R1 (MPa)	21.70	R1 (MPa)	20.60	R1 (MPa)	22.30
R2 (MPa)	37.20	R2 (MPa)	38.50	R2 (MPa)	39.00
R3 (MPa)	48.10	R3 (MPa)	46.10	R3 (MPa)	45.60

Source: Partner cement industry, 2019.

Moreover, Table 4 shows that the chemical composition of the cements reveals no significant differences between the evaluated oxides that could impact the cement reactions. Therefore, the composition of the calcium sulfate source (100% NG, 50/50% NG and PG, 100% PG) appears to be solely responsible for the behavior and properties observed in the results shown in Table 3.

Table 4 - Chemical composition of cements in % of oxides

CEM I	SiO_2	Al_2O_3	Fe_2O_3	CaO	MgO	SO_3	Na_2O	K_2O
	19.44	5.46	2.64	59.12	2.99	4.15	0.28	0.84
CEM II	SiO_2	Al_2O_3	Fe_2O_3	CaO	MgO	SO_3	Na_2O	K_2O
	19.92	5.28	2.74	58.37	3.56	4.11	0.29	0.8
CEM III	SiO_2	Al_2O_3	Fe_2O_3	CaO	MgO	SO_3	Na_2O	K_2O
	20.21	5.51	2.71	58.16	3.49	3.98	0.31	0.84

Source: Partner cement industry, 2019.

Regarding the sand (fine aggregate), the results are presented in Table 5. The data show that 85% of the particles are greater than 300 microns, and that the maximum dimension is 4.8 mm, which is standard for use in concrete mix. The coarse aggregate has a maximum size of 19 mm, and its characteristic data are presented in Table 6. Additionally, the granulometry distribution of the coarse aggregate meets the standard requirements for use in concrete mixtures.

Table 5 - Fine Aggregate Characterization

Sieve	% Average Retained	% Average Accumulated
#6.3	0%	0%
#4.8	2%	2%
#2.4	4%	6%
#1.2	9%	15%
#0.6	17%	32%
#0.3	53%	85%
#0.15	14%	99%
Bottom	1%	100%
Fineness Modulus		**2.38**
Maximum dimension (mm)		**4.8**
Bulk density ρap [kg/m³]		**1520**
Specific Gravity d3 [kg/m³]		**2470**

Table 6 - Coarse Aggregate Characterization

Sieve	% Average Retained	% Average Accumulated
#25	0%	0%
#19	3%	3%
#12,5	75%	78%
#9,5	21%	99%
Bottom	1%	100%
Fineness Modulus		**0,01**
Maximum dimension (mm)		**19mm**
Bulk density ρap [kg/m³]		**1620**
Average length C [mm]		**21,77**
Average thickness E [mm]		**11,35**
Shape Index		**1,92**

3.2 Isothermal calorimetry

Figure 5 illustrates the heat flow and accumulated heat release of CEM I samples with three different chloride addition levels. Analysis shows that chlorides increase heat release, especially in the early stages of the reaction (up to 40 hours). This is evidenced by the greater intensity of the main peak associated with the silicate reaction in the CEM I-II and CEM I-III mixes compared to CEM I-I, indicating an accelerated reaction. Li et al. (2021) suggested that chloride ions accelerate hydration reactions during nucleation and crystal growth.

The CEM I-II and CEM I-III pastes reached peaks of 2.71 and 2.63 mW/g of cement after 7.6 and 7.7 hours from the start of the reaction, respectively. In contrast, the mix without chloride addition peaked approximately 48 minutes later than CEM I-II, with about 14% less heat release (2.27 mW/g).

Significant accumulated heat values at early ages were observed at 24 hours: 165.03 J/g for CEM I-I, 174.13 J/g for CEM I-II, and 174.41 J/g for CEM I-III. Chloride presence accelerated the reaction, though there were no significant differences in results among the different chloride levels. Rodrigues Lago et al. (2017) showed that lower NaCl contents (up to 10% by mass of water) accelerate hydration reactions, while dosages above 20% delay reactions.

Figure 5 also indicates that the total accumulated heat after 72 hours showed no significant variations among the chloride levels. CEM I-II had a slightly higher accumulated heat (approximately 236.88 J/g of cement) compared to CEM I-I (about 232.68 J/g). Zhu et al. (2023) emphasized that the influence of chloride salts is highly dependent on the type of cation they are associated with.

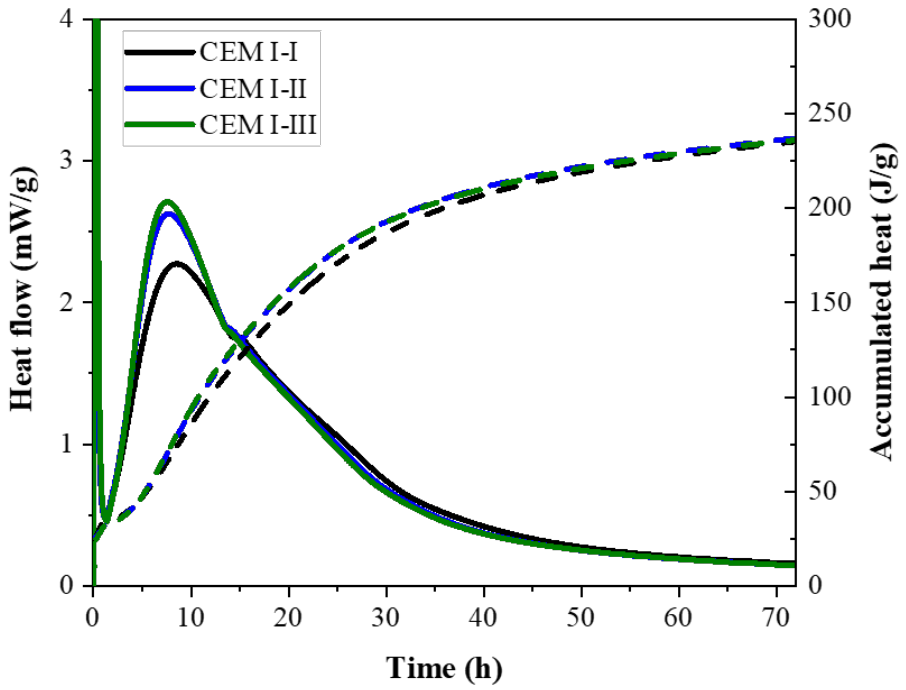

Figure 5 – Heat flow and accumulated heat: CEM I

Figure 6 displays the heat flow curves for CEM II blended cements, revealing two distinct peaks. The first peak, known as the main hydration peak, corresponds to the initial hydration reactions that contribute to the establishment and early strength development of the cement. The second peak is associated with sulfate depletion, the resumption of tricalcium aluminate activity, and monosulfate formation, as defined by ASTM C1679 (2017) and explained by Andrade Neto *et al.* (2021b).

Analysis of these curves indicates that cements containing PG tend to reach the

peak associated with the depletion of the calcium sulfate source earlier. Additionally, Figure 6 shows that for CEM II pastes, the difference between peaks with and without chloride addition increases. In contrast, as seen in Figure 5, CEM I did not exhibit a significant difference in the timing of the sulfate depletion peak.

The first heat peak can be observed after 9.20 hours, reaching 2.79 mW/g for CEM II-III, and after 9.86 hours, reaching 2.66 mW/g for CEM II-II. However, for sample CEM II-I, the first peak occurred only after 11.16 hours from the start of reactions (2.64 hours after the peak obtained by the 100% gypsum mix already mentioned, also without chlorides), with a heat flow of 2.26 mW/g. This result indicates a delay in setting rate caused by the use of PG, even as a partial substitute.

On the other hand, the released heat flow remained similar when comparing mixes without chloride additions. Furthermore, the accumulated heat curves show a greater influence of chlorides in blended cements. In the analysis of accumulated heat at 24 hours of reaction, the values obtained were 157.15 J/g for CEM II-I paste, 177.39 J/g for CEM II-II, and 181.58 J/g for CEM II-III, similar to gypsum cement values. After 72 hours, the values remained similar to gypsum-only cements, except for the composite cement mix without chlorides, which showed a lower value of 229.24 J/g (Figure 6).

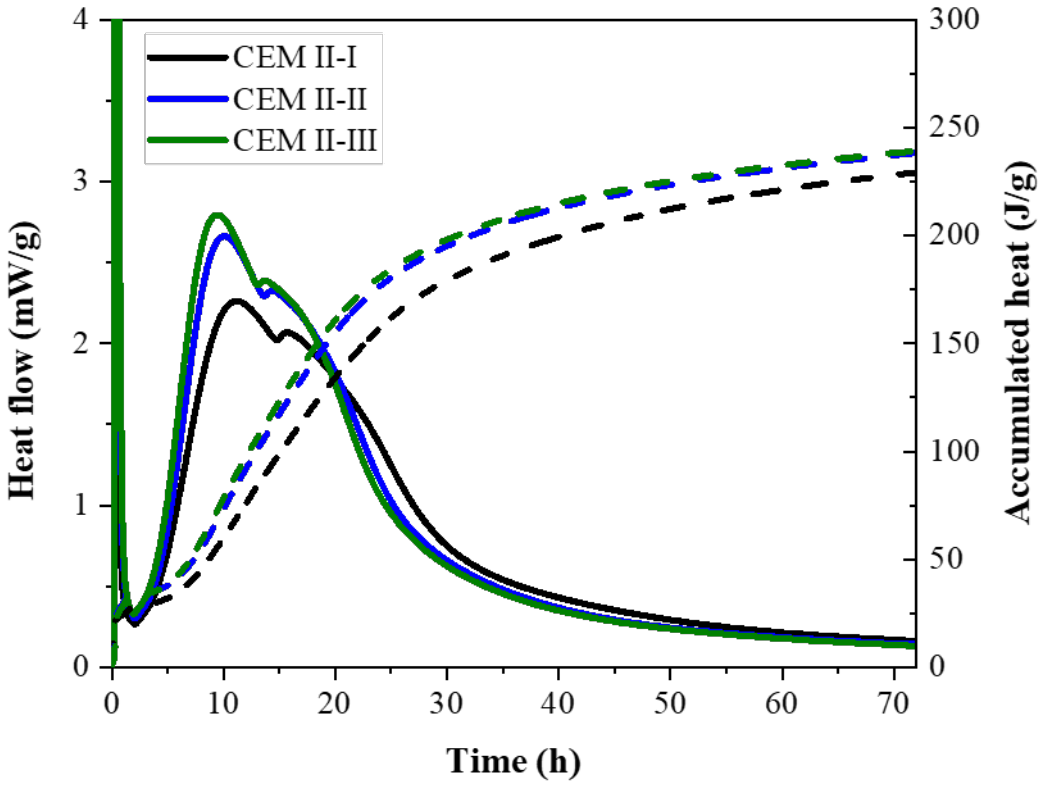

Figure 6 – Heat flow and accumulated heat: CEM II

When analyzing CEM III cements, as shown in Figure 7, peaks are observed occurring at 9.64 hours with 2.85 mW/g (for CEM III-III), 10.44 hours with 2.68 mW/g (for CEM III-II), and 11.60 hours with 2.29 mW/g (for CEM III-I). These results

indicate a delayed setting compared to CEM I mixes. However, after 24 hours, the accumulated heat values for these cements are significantly lower, with 126.69 J/g for CEM III-I, 137.79 J/g for CEM III-II, and 143.87 J/g for CEM III-III, representing reductions between 17% and 23% when compared to the reference pastes, CEM I.

After 72 hours, these cements show a considerable reduction compared to the reference cements (NG), even in the presence of chlorides, with values ranging from 204.29 to 206.92 J/g.

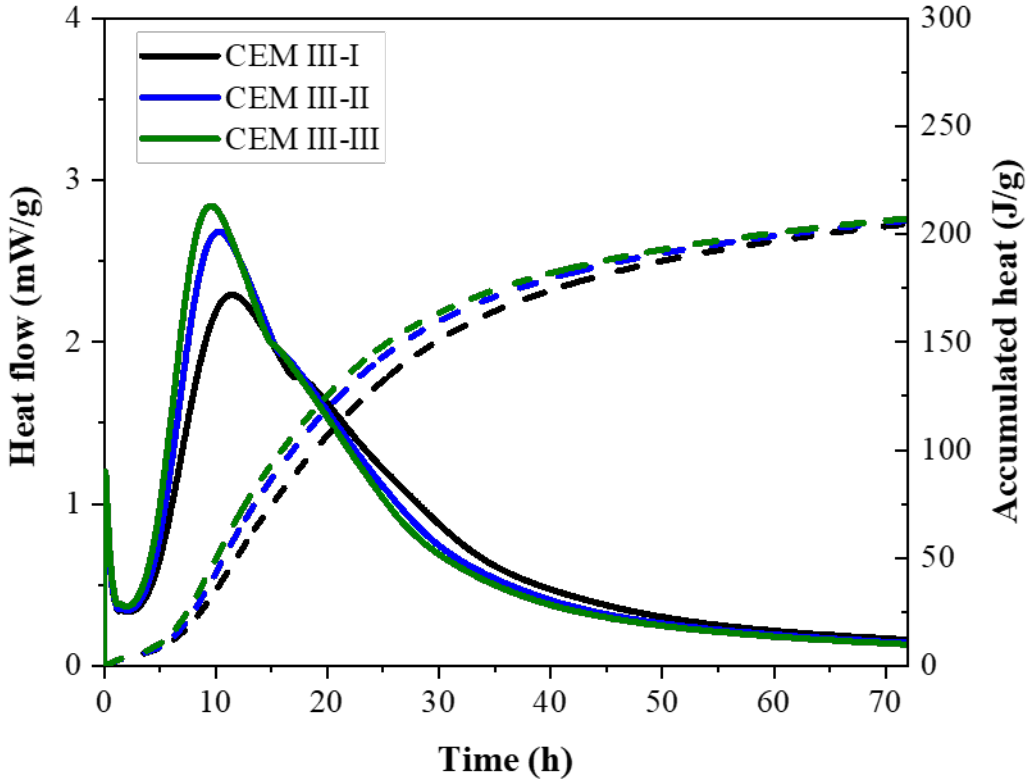

Figure 7 – Heat flow and accumulated heat: CEM III

ASTM C1679-17 (2017) defines initial setting time as the moment when 50% of the heat flow of the first peak is reached. Thus, the setting times for each mix were determined as shown in Table 7. The analysis reveals that, although the heat flow peaks do not vary significantly with PG substitution, the initial setting times are considerably affected by both the presence of chlorides and the comparison between mixes with and without phosphogypsum addition. These results corroborate previous studies indicating that impurities in PG can cause a significant delay in cement setting (Costa, 2022; Andrade Neto *et al.*,2021a; Holanda, Schmdit, Quarcioni, 2017).

Table 7 – Initial setting time (h) - Calculated by heat flow curves

CEM I-I	CEM I-II	CEM I-III	CEM II-I	CEM II-II	CEM II-III	CEM III-I	CEM III-II	CEM III-III
3.47	3.56	3.65	6.24	5.81	5.41	6.62	6.38	5.90

3.3 Slump of Concrete

The slump values obtained through the cone slump test, performed immediately after mixing, are presented in Table 8.

Table 8 - Slump test results (mm)

CEM I-I	CEM I-II	CEM I-III	CEM II-I	CEM II-II	CEM II-III	CEM III-I	CEM III-II	CEM III-III
120	110	120	125	130	125	140	130	140

It is observed that the mixes containing conventional cements (CEM I) have an average slump of 116.6 mm. The mixes with blended cements (CEM II) show an average of 126.6 mm. Finally, the mixes with total substitution of gypsum by phosphogypsum (CEM III) have an average slump of 136.6 mm. It is noted that the addition of sodium chloride did not cause changes that could indicate a behavioral trend. These results demonstrate that the alteration in the source of calcium sulfate in cement resulted in a linear increase in slump, providing greater fluidity to the concrete.

3.4 Compressive Strength

The specimens from the nine concrete mixes were tested at ages of 1, 7, and 28 days to analyze the evolution of compressive strengths, as presented in Figure 8.

Analyzing the cements without chloride additions, Figure 8 shows that the best results are attributed to CEM II cement, achieving 16.69 MPa, 25.87 MPa, and 28.97 MPa at 1, 7, and 28 days, respectively. In contrast, CEM I-I cement shows the lowest results at all ages compared to the other mixes without chlorides. This scenario indicates that the PG used in this study is of high quality, with low impurity content.

However, the presence of 0.15% chlorides alters this trend, favoring the performance of pure cement (CEM I), as evidenced in the results. For mixes with 0.30% chlorides, behaviors vary across ages, with notable performance by blended cement (CEM II), reaching 30.09 MPa at 28 days. Shi *et al.* (2016) reported in their study that increased addition of NaCl resulted in higher rates of compressive strength development.

In the age analysis in Figure 8, it is observed that at 1 day, CEM II-III mix

achieved the best result. Regarding the effects of chlorides, variations in behaviors are observed for each type of cement: for CEM I, chlorides showed benefits only at the 0.15% level; for other cements, this relationship reverses, with the highest strengths observed in concretes with 0.30% chlorides.

At 7 days, as presented in Figure 8, trends remain consistent for CEM I cement, while for other mixes, there is a slight increase in average strengths in mixes without chlorides compared to 0.15% levels. In mixes with 0.30% chlorides, the results continue to show the highest strengths.

At 28 days, as shown in Figure 8, it is evident that gypsum cement remains the most affected by the presence of chlorides. Once again, CEM I-II mix stands out with the highest average strength of 31.17 MPa. For PG cements, a consistent pattern is observed, with blended mixes showing the best results.

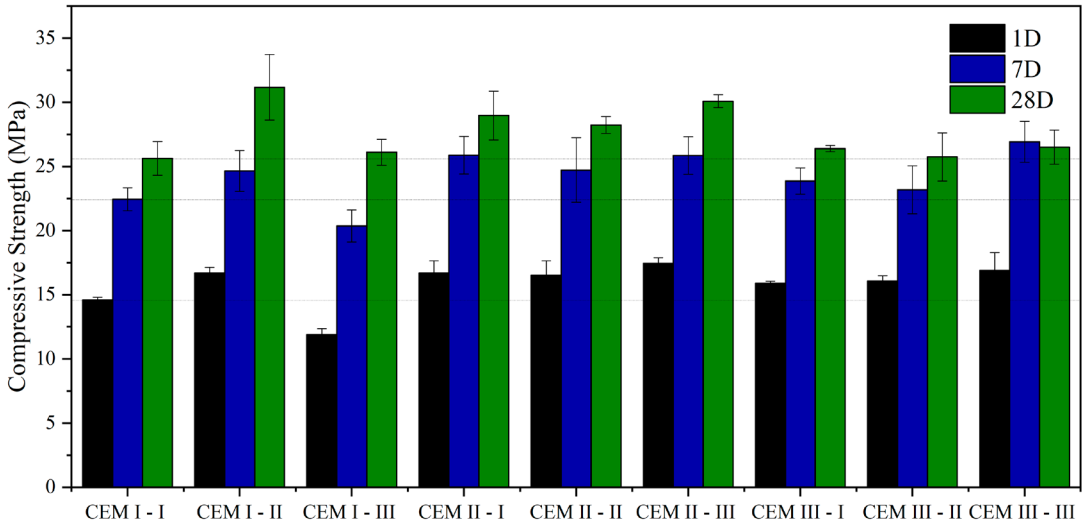

Figure 8 – Compressive strength [MPa]

In general, it is observed that the presence of chlorides did not have a significant impact on the average compressive strengths. On the other hand, cements with partial replacement of gypsum by phosphogypsum (CEM II) showed superior results to CEM I cement, including at early ages. This result is consistent with the values of accumulated heat observed in calorimetry analyses, especially after 24 hours of hydration.

However, the specimens from the CEM I-III mix showed an atypical behavior, with lower compressive strengths at all ages. Therefore, regarding compressive strength, the use of phosphogypsum as a source of calcium sulfate in cement production proves to be viable. On the other hand, the addition of chlorides did not show significant benefits in the compressive strengths studied in concrete from the first day of curing.

3.5 Corrosion Potential

Figure 9 shows the results of the mix design without the use of chlorides for the three different cements. It is observed that in the first three weeks, the values fluctuate within the uncertain probability range of corrosion. However, from the fourth to the eighth week, the values stabilize in the low probability range of corrosion, with results above -85mV. Therefore, the results indicate that all cements without chlorides present a low probability of corrosion, considering this time interval.

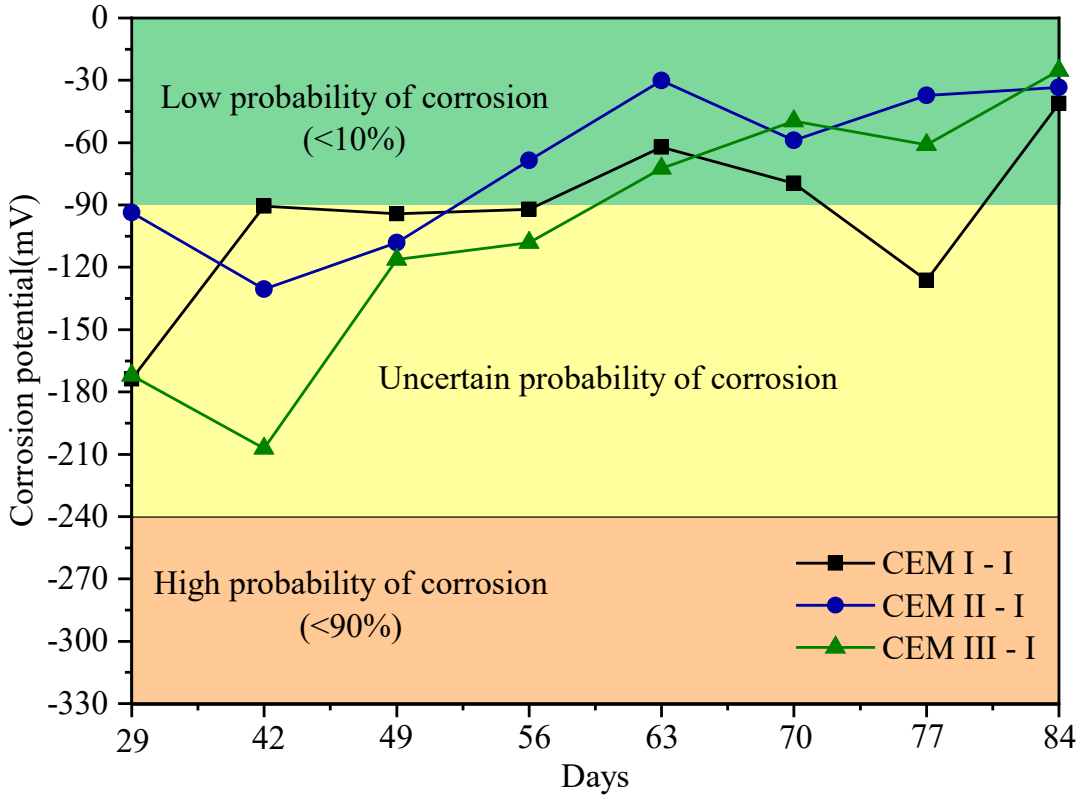

Figure 9 – Corrosion Potential in 0% Chloride Traces

In Figure 10, it is observed that for the mixes with addition of 0.15% chloride, the cements CEM I-II and CEM II-II achieve stability in the low probability range of corrosion from the third week of testing onwards. However, the mix with CEM III-II shows results in the uncertain probability range of corrosion for six out of the eight testing weeks, indicating a point of concern due to the inconclusiveness of the results during this period.

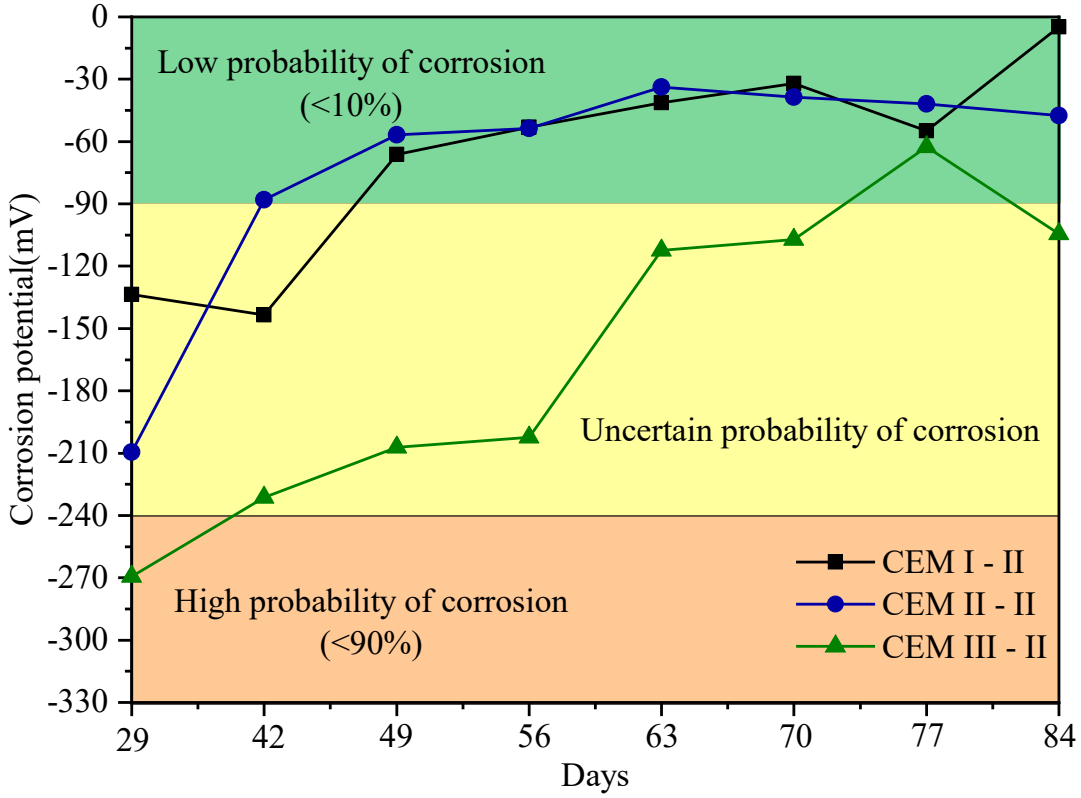

Figure 10 – Corrosion Potential in 0.15% Chloride Traces

In Figure 11, traces with the addition of 0.30% chlorides, from the third week onwards, a trend of curve stabilization is observed for CEM II-III and CEM III-III cements. However, the results remain close to the -85mV range, transitioning between uncertain and low probability of corrosion. Comparatively, Theiss (2019) also found results close to this range for up to 12 weeks when studying CP II F 40 cements in specimens with 25mm cover. In contrast, Cabral (2000) obtained results indicating a high probability of corrosion for CP II F 32 mixes with 10mm cover at the same age. It is important to note that comparative studies employed the accelerated testing method with chloride attack cycles, which differs from the approach of this study that included chlorides in the mix composition. Ferenc et al (2024) points out that the impact of chlorides on reinforcement is more intense and alarming when the reinforcement is exposed to chloride solutions, as reported in the study that exposed it to a 3.5% NaCl solution. Given the high variability of the data obtained in this test, the results should be interpreted cautiously.

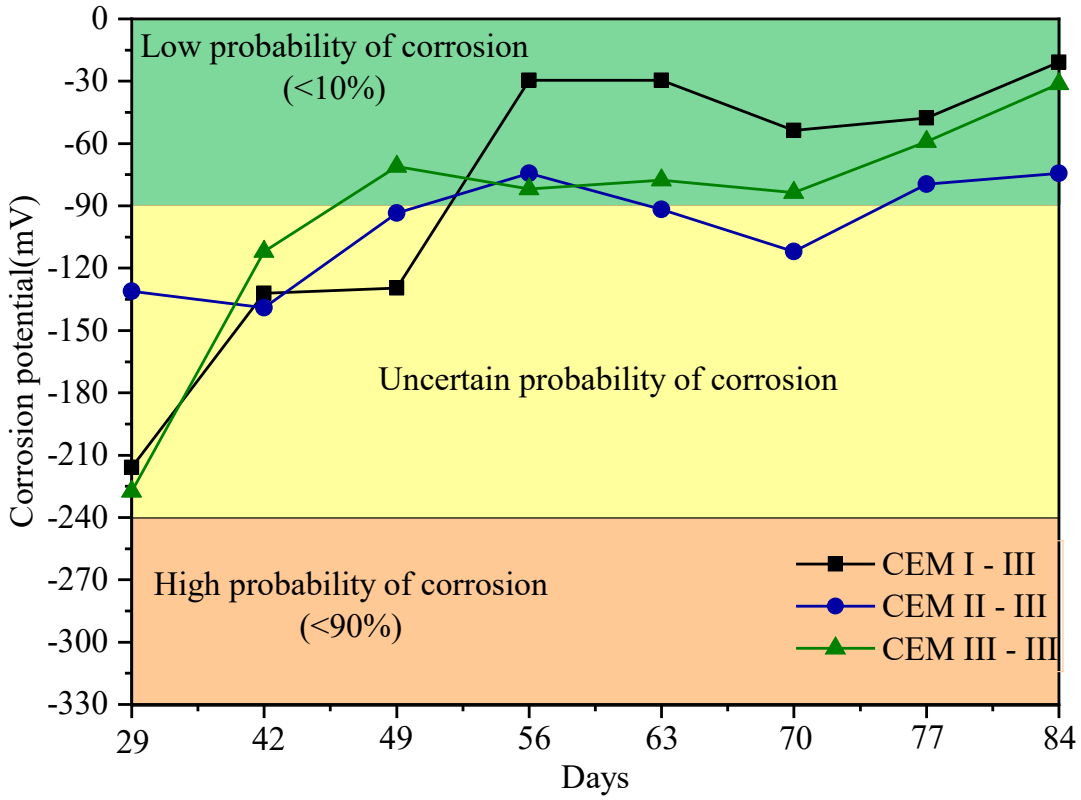

Figure 11– Corrosion Potential in 0.30% Chloride Traces

4 Conclusion

This study aimed to analyze the effects of partial or total replacement of gypsum (NG) with phosphogypsum (PG) as a setting regulator in the cement industry. The research evaluated pastes and concretes using three compositions: CEM I (100% gypsum), CEM II (50% gypsum + 50% phosphogypsum), and CEM III (100% phosphogypsum), combined with three different sodium chloride contents (0%, 0.15%, and 0.30%), used as reaction accelerators. The mixes underwent calorimetry tests, compressive strength tests, and corrosion potential tests.

The results indicate that phosphogypsum causes significant changes in the hydration reaction of cements, such as increased setting time and delayed peaks of silicates, as evidenced by calorimetry tests. Moreover, cements containing phosphogypsum showed an early peak depletion of sulfates. In concrete, the use of this residue did not negatively affect compressive strength, demonstrating values superior to gypsum cements, especially at early ages.

However, the study confirms previous findings indicating excessive setting delay when using phosphogypsum, as observed in initial setting times. On the other hand, the addition of chlorides proved effective in mitigating the effects of phosphogypsum,

accelerating hydration peaks. Nevertheless, there was a 2.43-hour difference in initial setting time between mixes with gypsum without chlorides and those with 100% phosphogypsum with the highest NaCl content.

References

AMERICAN SOCIETY FOR TESTING AND MATERIALS. C876-15: *Standard Test Method for Corrosion Potentials of Uncoated Reinforcing Steel in Concrete*. 2015.

AMERICAN SOCIETY FOR TESTING AND MATERIALS. C876-15: *Standard Test Method for Corrosion Potentials of Uncoated Reinforcing Steel in Concrete*. 2015.

American Society for Testing Materials. *ASTM C1679-08. Measuring Hydration Kinetics of Hydraulic Cementitious Mixtures Using Isothermal Calorimetry.* West Conshohocken, 2017.

ASSOCIAÇÃO BRASILEIRA DE CIMENTO PORTLAND. *NBR 16606: Cimento Portland - Determinação da pasta de consistência normal*. Rio de Janeiro, 2019a.

ASSOCIAÇÃO BRASILEIRA DE CIMENTO PORTLAND. *NBR 16607: Cimento Portland - Determinação dos tempos de pega.* Rio de Janeiro, 2018.

ASSOCIAÇÃO BRASILEIRA DE NORMAS TÉCNICAS. *NBR 11579: Cimento Portland — Determinação do índice de finura por meio da peneira de 75 μm (nº 200).* Rio de janeiro, 2015b.

ASSOCIAÇÃO BRASILEIRA DE NORMAS TÉCNICAS. *NBR 12655: Concreto de cimento Portland - Preparo, controle, recebimento e aceitação- Procedimento*. Rio de Janeiro, 2015.

ASSOCIAÇÃO BRASILEIRA DE NORMAS TÉCNICAS. *NBR 16372. Cimento Portland e outros materiais em pó - Determinação da finura pelo método de permeabilidade ao ar (Método Blaine)*. Rio de Janeiro, 2015.

ASSOCIAÇÃO BRASILEIRA DE NORMAS TÉCNICAS. *NBR 16889: Concreto - Determinação da consistência pelo abatimento do tronco de cone.* Rio de Janeiro, 2020.

ASSOCIAÇÃO BRASILEIRA DE NORMAS TÉCNICAS. *NBR 248: Agregados - Determinação da composição granulométrica.* Rio de Janeiro, 2003.

ASSOCIAÇÃO BRASILEIRA DE NORMAS TÉCNICAS. *NBR 45: Agregados – Determinação da massa unitária e do volume de vazios.* Rio de Janeiro, 2006.

ASSOCIAÇÃO BRASILEIRA DE NORMAS TÉCNICAS. *NBR 52: Agregado miúdo – Determinação da massa específica e massa específica aparente.* Rio de Janeiro, 2009.

ASSOCIAÇÃO BRASILEIRA DE NORMAS TÉCNICAS. *NBR 5739: Concreto - Ensaio de compressão de corpos de prova cilíndricos.* Rio de Janeiro, 2018.

ASSOCIAÇÃO BRASILEIRA DE NORMAS TÉCNICAS. *NBR 7215. Cimento Portland - Determinação da resistência à compressão de corpos de provas cilíndricos*. Rio de Janeiro, 2019.

ASSOCIAÇÃO BRASILEIRA DE NORMAS TÉCNICAS. *NBR 7809: Agregado graúdo - Determinação do índice de forma pelo método do paquímetro - Método de ensaio*. Rio de Janeiro, 2019.

ASSOCIAÇÃO BRASILEIRA DE NORMAS TÉCNICAS. *NM18. Cimento Portland - Análise química - Determinação de perda ao fogo.* Rio de Janeiro, 2012.

AKFAS, F. et al. Exploring the potential reuse of phosphogypsum: A waste or a resource? *Science of the total environment*, v. 908, p. 168196, 2024.

ANDRADE NETO, J. da S.; DE LA TORRE, A. G.; KIRCHHEIM, A. P. Effects of sulfates on the hydration of Portland cement – A review. *Construction and Building Materials*, v. 279, p. 122428, 2021b.

ANDRADE NETO, J. S. et al. Influence of phosphogypsum purification with lime on the properties of cementitious matrices with and without plasticizer. *Construction and Building Materials*, v. 299, p. 123935, 2021a.

BALTAR, C. A. M.; LUZ, A. B. D.; BASTOS, F. D. F. *Diagnóstico do Pólo Gesseiro de Pernambuco (Brasil) com ênfase na produção de Gipsita para fabricação de Cimento.* Tegucigalpa, Honduras, 2004.

BAUER, L. A. Falcão. *Materiais de Construção.* 5ª ed. Revisada, Rio de Janeiro, 2000.

Brasil. Rio de Janeiro: CETEM/MCT, 2010. Cap. 7, p. 125–144.

CABRAL, Antônio Eduardo Bezerra. *Avaliação da eficiência de sistemas de reparo no combate à iniciação e à propagação da corrosão do aço induzida por cloretos.* Dissertação (Mestrado em Engenharia) – Programa de Pós-Graduação em Engenharia Civil. Porto Alegre, 2000.

CABRAL, Antônio Eduardo Bezerra. *Avaliação da eficiência de sistemas de reparo no combate à iniciação e à propagação da corrosão do aço induzida por cloretos.* Dissertação (Mestrado em Engenharia) – Programa de Pós-Graduação em Engenharia Civil. Porto Alegre, 2000.

CANUT, M. M. C. et al. Microstructural analyses of phosphogypsum generated by Brazilian fertilizer industries. *Materials Characterization*, v. 59, n. 4, p. 365–373, 2008.

CAO, J. et al. Promoting coordinative development of phosphogypsum resources reuse through a novel integrated approach: A case study from China. *Journal of Cleaner Production*, v. 374, p. 134078, 2022a.

COSTA, R. P. et al. Effect of soluble phosphate, fluoride, and pH in Brazilian phosphogypsum used as setting retarder on Portland cement hydration. *Case Studies in Construction Materials*, v. 17, p. e01413, 2022.

CUI, Y. et al. A systematic review of phosphogypsum recycling industry based on the survey data in China-applications, drivers, obstacles, and solutions. *Environmental Impact Assessment Review,* v. 105, p. 107405, 2023.

FEREC, T., WOJTCZAK, E., MERONK, B., RUCKA, M. Characterization of corrosion in reinforced concrete beams using destructive and non-destructive tests. *Case Studies in Construction Materials.* v 20, e03309, 2024.

GODINHO, J. P.; OLIVEIRA, R. L. N.; CAPRARO, A. P. B.; RÉUS G. C.; MEDEIROS, M. H. F. *Influência das condições de limpeza de barras de aço carbono do concreto armado nas leituras eletroquímicas de densidade de corrente de corrosão e potencial de corrosão.* In: ENCONTRO

LUSO-BRASILEIRO DE DEGRADAÇÃO EM ESTRUTURAS DE CONCRETO ARMADO, 3., São Carlos, 2018.

HANEKLAUS, N. et al. Closing the upcoming EU gypsum gap with phosphogypsum. Resources, Conservation and Recycling. *Resources, Conservation & Recycling*, v. 182, 2022.

HERMANN, L.; KRAUS, F.; HERMANN, R. Phosphorus processing-potentials for higher efficiency. *Sustainability (Switzerland)*, v. 10, n. 5, 2018.

HOLANDA, F. DO C.; SCHMIDT, H.; QUARCIONI, V. A. Influence of phosphorus from phosphogypsum on the initial hydration of Portland cement in the presence of superplasticizers. *Cement and Concrete Composites*, v. 83, p. 384–393, 2017.

ISLAM, G M Sadiqul et. al. Effect of Phosphogypsum on the Properties of Portland Cement. *Procedia Engineering*, v. 171, p. 744–751, 2017.

KIRCHHEIM, A. P. et al. Álcalis incorporados ao aluminato tricálcico: efeitos na hidratação alkalis incorporated into tricalcium aluminate: effects in hydration. *Ambiente Construído*, v. 10, n. 1, p. 177–189, 2010.

KUZMANOVIĆ, P.; TODOROVIĆ, N.; FORKAPIĆA, S.; PETROVIĆ, L. F.; KNEŽEVIĆ, J.; NIKOLOV, J.; MILJEVIĆ, B. *Radiological characterization of phosphogypsum produced in Serbia*. Radiation Physics and Chemistry, 2020.

LEE, Taegyu; LEE, Jaehyun; KIM, Yongro. *Effects of admixtures and accelerators on the development of concretestrength for horizontal form removal upon curing at 10°C.* Construction and Building Materials, v. 237, 2020.

LI, W. et al. Effects of Seawater, NaCl, and Na_2SO_4 Solution Mixing on Hydration Process of Cement Paste. *Journal of Materials in Civil Engineering*, v. 33, n. 5, 2021.

MEHTA, P. K.; MONTEIRO, P. J. M. *Concrete. Microstructure, properties and materials*. 3 ed., McGraw-Hill, 2014.

MOTA, Daniel Andrade. *Influência da adição de materiais pozolânicos na corrosibilidade do concreto armado, analisada por meio do potencial de corrosão e resistividade elétrica*. Dissertação (Mestado em Engenharia Ambiental Urbana) – Escola Politécnica, UFBA, Salvador, 2016.

MYRDAL, Roar. *Accelerating admixtures for concrete*. SINTEF Building and Infrastructure, 2007.

RASHAD, Alaa M. *Phosphogypsum as a construction material.* Journal of Cleaner Production, v. 166, p. 732-743, 2017.

REN, Guosheng; TIAN, Zhijie; WU, Jingjiang; GAO, Xiaojian. *Effects of combined accelerating admixtures on mechanical strength and microstructure of cement mortar.* Construction and Building Materials, v. 304, 2021.

RIBEIRO, D. V.; CUNHA, M. P. T. Técnicas de avaliação e monitoramento da corrosão em estruturas de concreto armado. In: RIBEIRO, Daniel Véras (org.). *Corrosão em Estruturas de Concreto Armado: Teoria, Controle e Métodos de Análise*. 1 ed. Rio de Janeiro: Elsevier, 2014, p. 296 - 397.

RODRIGUES LAGO, F. et al. Evaluation of Influence of Salt in the Cement Hydration to Oil Wells. *Materials Research*, v. 20, p. 743–747, 2017.

SHEN, W. *et al. Utilization of solidified phosphogypsum as Portland cement retarder.* Journal of Material Cycles and Waste Management, [s. l.], v. 14, n. 3, p. 228–233, 2012.

SHI, Z. *et al*. Effects of triisopropanol amine, sodium chloride and limestone on the compressive strength and hydration of Portland cement. *Construction and Building Materials.* v 125, p 210-218, 2016.

SILVA, R. M.; GIULIETTI, M. Fosfogesso: geração, destino e desafios. In: *Agrominerais.* CETEM/MCT, 2010

THEISS, Ana Flávia. *Avaliação da corrosão do aço em concreto com adição de inibidor migratório de corrosão frente à ação de íons cloreto.* Dissertação (Mestrado em Engenharia Civil) – Programa de Pós-Graduação em Engenharia Civil do Centro de Ciências Tecnológicas, UESC, Joinville, 2019.

VIEIRA, G.L. *Estudo do processo de corrosão sob a ação de íons cloreto em concretos obtidos a partir de agregados reciclados de resíduos de construção e demolição.* Dissertação (Mestado em Engenharia) – Programa de Pós Graduação em Engenharia Civil, UFRGS, Porto Alegre, 2003.

ZHU, G. et al. Effects of chloride salts on strength, hydration, and microstructure of cemented tailings backfill with one-part alkali-activated slag. *Construction and Building Materials,* v. 374, p. 130965, 2023.